Water transport in protoplanetary disks and the hydrogen isotopic composition of chondrites

Emmanuel Jacquet[a,b,*], François Robert[b]

[a] *Canadian Institute for Theoretical Astrophysics, University of Toronto, 60 St Georges Street, Toronto, ON M5S 3H8, Canada*
[b] *Laboratoire de Minéralogie et de Cosmochimie du Muséum, CNRS & Muséum National d'Histoire Naturelle, UMR 7202, 57 rue Cuvier, 75005 Paris, France.*

Abstract

The D/H ratios of carbonaceous chondrites, believed to reflect the hydrogen isotopic composition of water in the inner early solar system, are intermediate between the protosolar value and that of most comets. The isotopic composition of cometary water has been accounted for by several models where the isotopic composition of water vapor evolved by isotopic exchange with hydrogen gas in the protoplanetary disk. However, the position and the large range of variation of the distribution of D/H ratios in carbonaceous chondrites have yet to be explained. In this paper, we assume that the D/H composition of cometary ice was achieved in the disk building phase and model the further isotopic evolution of water in the inner disk in the classical T Tauri stage. Reaction kinetics compel isotopic exchange between water and hydrogen gas to stop at ~500 K, well inside the snow line. However, the equilibrated water can be transported to the snow line (and beyond) via turbulent diffusion and consequently mix with isotopically comet-like water. Thus the competition between outward diffusion and net inward advection established an isotopic gradient, which is at the origin of the large isotopic variations in the carbonaceous chondrites and other water-bearing objects accreted in the protoplanetary disk.

Under certain simplifying assumptions, we calculate analytically the probability distribution function of the D/H ratio of ice accreted in planetesimals and compare it with observational data. The distribution is found to essentially depend on two parameters: the radial Schmidt number Sc_R, which ratios the efficiencies of angular momentum transport and turbulent diffusion, and the range of heliocentric distances over which currently sampled chondrite parent bodies were accreted. The minimum D/H ratio of the distribution corresponds to the composition of water condensed at the snow line, which is a function of both the composition of equilibrated water having diffused from hotter disk regions and the efficiency of this outward transport as measured by Sc_R. Observations constrain the latter to low values (0.1-0.3), which suggests that turbulence in the planet-forming region was hydrodynamical in nature, as would be expected in a dead zone. Such efficient outward diffusion would also account for the presence of high-temperature minerals in comets.

Keywords: Meteorites, Solar nebula, Cosmochemistry, Disk, Comets

1. Introduction

The isotopic composition of hydrogen (as expressed by the D/H ratio) is a valuable tracer of the origin of water in the solar system (Robert 2006). Primitive meteorites (*chondrites*), presumably the building blocks of terrestrial planets, allow a glimpse at the D/H ratio of water in the protoplanetary disk that surrounded our Sun 4.57 Ga ago. Indeed, many chondrites, in particular *carbonaceous chondrites*, contain clays formed through alteration of originally anhydrous silicates by water presumably incorporated as ice along with rock during accretion (Brearley 2003; Ghosh *et al.* 2006).

The measured D/H ratios of bulk carbonaceous chondrites[1] (see Fig. 5), generally thought to reflect that of accreted water (but see Alexander *et al.* 2012b), span a range of 120×10^{-6} to 230×10^{-6} (excluding CR chondrites). The distribution, which is skewed to heavy isotopic compositions, has a mean $(156 \pm 3) \times 10^{-6}$ close to the $(149 \pm 3) \times 10^{-6}$ estimated for the bulk Earth (Lécuyer *et al.* 1998) — consistent with a chondritic source for terrestrial water. The D/H ratios of carbonaceous chondrites is systematically lower than that exhibited by many Oort-cloud comets ($(296 \pm 25) \times 10^{-6}$; Hartogh *et al.* 2011), although D/H ratios of $(161 \pm 24) \times 10^{-6}$ and $(206 \pm 22) \times 10^{-6}$ have been determined for Jupiter-family comet Hartley 2 and Oort-cloud comet Garradd, respectively (Hartogh *et al.* 2011; Bockelée-Morvan *et al.* 2012). The composition of interplanetary dust particles, though broadly similar to that of carbonaceous chondrites (e.g. Engrand and Maurette 1998; Bradley 2005), has a significant tail extending to cometary values and beyond. Both chondritic and cometary domains of variation are markedly distinct from both the estimated protosolar value ($(20 \pm 3.5) \times 10^{-6}$; Geiss and Gloeckler 2003), dominated by the isotopic composition of hydrogen gas, and the high values ($\mathrm{D/H} \gtrsim 10^{-3}$) determined in molecular clouds for molecules other than H_2, consistent with predictions from ion-molecule

*Corresponding author
Email address: ejacquet@cita.utoronto.ca (Emmanuel Jacquet)

[1] And carbonaceous chondrite-like microclasts in howardites (Gounelle *et al.* 2005).

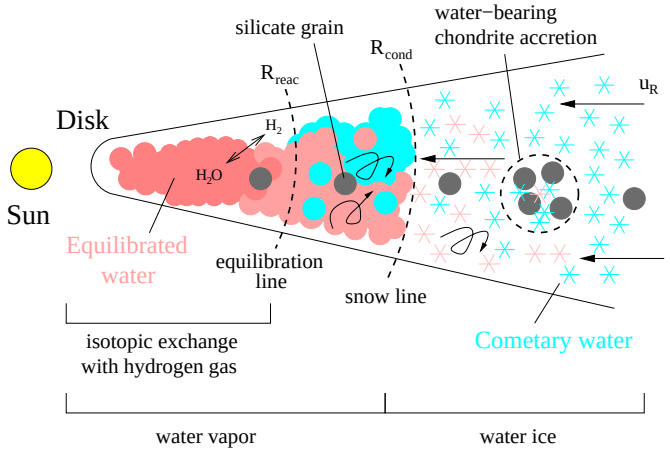

Figure 1: Cartoon of the model investigated here. We distinguish between (comet-like) "cometary water" (cyan) and "equilibrated water" (pink) that has undergone isotopic exchange with the hydrogen gas inside the "equilibration line" ($R_{\rm reac}$). Water is gaseous inside the snow line ($R_{\rm cond}$) and solid beyond (as symbolized by the cloud and snowflakes symbols, respectively). Accretion of water as ice occurs beyond the snow line. Arrows symbolize motions of the gas.

reactions (see e.g. Robert 2006). However, high D/H values $\gtrsim 2\times10^{-3}$ have been reported at the micrometer scale in clays of the Semarkona chondrite (Piani *et al.* 2012; Piani 2012) and may reflect the composition of pristine interstellar ice grains.

In the protoplanetary disk, the D/H ratio of water evolves mainly through isotopic exchange with the hydrogen gas (whose composition remains essentially fixed at the protosolar value because it contains the bulk of the H of the system), that is, via the reaction:

$$\mathrm{HDO} + \mathrm{H_2} \leftrightarrows \mathrm{H_2O} + \mathrm{HD} \qquad (1)$$

The equilibrium fractionation factor $(\mathrm{D/H})_{\mathrm{H_2O}}/(\mathrm{D/H})_{\mathrm{H_2}}$ is unity at high temperatures ($\gtrsim$ 1000 K), but increases with decreasing temperature (Richet *et al.* 1977).

Using one-dimensional disk models, Drouart *et al.* (1999) showed that reaction (1) was unable to account for the chondritic or cometary D/H ratios if water was assumed to have formed in the protoplanetary disk with the protosolar D/H value. Indeed reaction kinetics would have been prohibitively slow in those cold regions of the disk where sufficient D enrichment would have been predicted by thermodynamic equilibrium. On the other hand, Drouart *et al.* (1999) found that cometary compositions could be obtained if water was inherited from the protosolar cloud (with heavy D/H $\sim 10^{-3}$). Water would have evolved toward isotopically lighter compositions in the inner disk and diffused in the colder regions owing to turbulence, a result also obtained by Mousis *et al.* (2000) and Hersant *et al.* (2001). Transport and mixing would have been particularly efficient in the early stages of disk evolution, if the disk was first built compact and then expanded because of turbulence (Yang *et al.* 2012). Such a picture is also consistent with the presence of crystalline silicates in comets (Bockelée-Morvan *et al.* 2002).

While these previous works focused on reproducing D/H value observed in comets, implications on the composition of water in the inner solar system, and in particular the fairly large domain of variations of the D/H ratio in chondrites have yet to be worked out in this framework. This is the purpose of this paper.

In this paper, we consider a disk model pertaining to the classical T Tauri phase, that is, after infall has ceased and the disk radius has become large compared to the heliocentric distances of interest. This is the epoch where chondrite accretion is believed to have taken place. At that time, the D/H ratio of water ice in the outer disk is assumed to have been already set and homogenized at the value of $\sim 300\times10^{-6}$ measured in most comets as a result of early disk processes (this would correspond to the plateau in the simulation of Yang *et al.* (2012), whose level varies little after infall has stopped). Close to the Sun, isotopic exchange between (gaseous) water and hydrogen gas (reaction (1)) is still going on. However, beyond a certain heliocentric distance (corresponding to a temperature of ~500 K, as we shall argue later), the kinetics of this reaction are so slow that essentially no isotopic exchange occurs there. Due to gas turbulence, however, some of the water equilibrated with H_2 sunward of this heliocentric distance will be transported outward and will reach the *snow line*, where ice condenses. Water beyond the snow line—sampled by chondrites—will thus be a mixture of two components: equilibrated water having diffused from the hot inner regions of the disk, and cometary water drifting inward from the outer disk.

A radial gradient in D/H ratio is thus established by the competition between outward diffusion and inward advection which sets the proportions of equilibrated water and cometary water as a function of heliocentric distance. The range of D/H ratios of water-bearing bodies thus extends from cometary compositions down to the composition of water condensed at the snow line. The composition sampled at the snow line is hence intermediate between cometary values and those expected from equilibration with H_2. This schematic description provides a framework to account for the fairly large variations of the D/H ratio in water of solar system bodies. A cartoon of the scenario is presented in Fig. 1.

The goal of this paper is to calculate analytically the distribution of D/H ratios of chondritic water that results from this picture and compare it to the observational data, in order to constrain the model parameters. In particular, the calculation will be constrained by the asymmetrical shape of the distribution and its position relative to cometary values. We stress that here the cometary value is a *starting*, observationally given parameter of the model. Our model does not aim at reproducing the composition of comets in contrast to the studies of Drouart *et al.* (1999); Mousis *et al.* (2000); Hersant *et al.* (2001); Yang *et al.* (2012) ; rather, in complementarity to those, it focuses on chondrite parent bodies, that is, the inner regions of the solar system. Also in complementarity to these numerical studies, our work, in being analytic in nature, allows us to nail down, under certain simplifying assumptions, the relevant parameters (essentially two) that govern the distribution of chondritic D/H ratios, namely: the range of heliocentric distances sampled by chondrites and the radial Schmidt number—which essentially ratios

the efficiencies of angular momentum transport and turbulent diffusion. We will find that low values of the radial Schmidt number yield D/H variations consistent with observations. The paper is organized as follows: We describe the model assumptions in Section 2, present and discuss the results in Sections 3 and 4, respectively. In Section 5, we conclude. For the sake of clarity, specific derivations are deferred to appendices.

2. Modeling

In this section, we introduce our notations and modeling principles. We successively consider the disk model (Section 2.1), the transport of water (Section 2.2), its D/H ratio (Section 2.3) and our prescription for accretion and delivery to Earth (Section 2.4).

2.1. The disk

We consider an axisymmetric, vertically isothermal turbulent disk. The disk is assumed to have a stationary surface density profile in its inner regions such that its (radially constant) mass accretion rate $\dot{M}$ is given by:

$$\dot{M} \equiv -2\pi R \Sigma u_R = 3\pi \Sigma \alpha \frac{c_s^2}{\Omega} \tag{2}$$

with R the heliocentric distance, Σ the surface density, u_R the vertically averaged radial velocity of the gas, α the vertically averaged turbulence parameter, Ω the Keplerian angular velocity and $c_s = \sqrt{k_B T/m}$ the isothermal sound speed—where k_B and m are the Boltzmann constant and the mean molecular mass, respectively, and T the temperature. The steady-state approximation is expected to hold so long the viscous evolution timescale,

$$t_{\rm vis}(R) \equiv \frac{R^2}{3\alpha c_s^2/\Omega} = 0.05 \text{ Ma } R_{\rm AU}^{1/2} \left(\frac{300 \text{ K}}{T}\right)\left(\frac{10^{-3}}{\alpha}\right), \tag{3}$$

is shorter than the disk's age in the regions of interest. Similarly to Drouart *et al.* (1999) and Hersant *et al.* (2001)—see also Hartmann *et al.* (1998) and Chambers (2009)—, we take the mass accretion rate to evolve in time as[2]

$$\dot{M} = \frac{\dot{M}_0}{(1 + t/t_0)^{3/2}} \tag{4}$$

where $\dot{M}_0$ is the mass accretion rate at some initial time $t = 0$ and t_0 an evolution timescale ($t_0 > t_{\rm vis}(R)$).

We adopt the same temperature prescription as in Jacquet *et al.* (2012):

$$T = \max\left[\left(\frac{3}{128\pi^2}\frac{\kappa m}{\sigma_{\rm SB} k_B \alpha}\dot{M}^2\Omega^3\right)^{1/5}, f_T T_0 R_{\rm AU}^{-1/2}\right], \tag{5}$$

with κ the specific opacity, $\sigma_{\rm SB}$ the Stefan-Boltzmann constant, $T_0 = 280$ K, f_T a dimensionless constant parameter (for which we will adopt a fiducial value of 0.5) and $R_{\rm AU} \equiv R/(1 \text{ AU})$. This prescription essentially states that inner disk regions are dominated by the dissipation of turbulence ("viscous heating"), which decreases with decreasing accretion rate, whereas the outer disk regions are dominated by reprocessing of solar radiation. Hence, the snow line (at heliocentric distance $R_{\rm cond}$), which corresponds to a fixed temperature of $T_{\rm cond}$=170 K, recedes toward the Sun with the passage of time.

For simplicity, we will assume that α and κ are constant throughout the disk's extent and evolution.

2.2. Water transport

We now turn to the transport of water. We distinguish between *nebular* and *accreted* water. *Nebular water* is water dynamically coupled to the gas, whether as water vapor or ice-bearing grains, and behaves as part of the disk. It is predominantly gaseous inside the snow line and solid outside it. *Accreted water* refers to water retrieved from the gas by incorporation in planetesimals or comets.

We first focus on the dynamics of nebular water. Since it behaves as a passive contaminant in the gas, the evolution equation of its surface density $\Sigma_{\rm H_2O}$ reads (e.g. Ciesla and Cuzzi 2006):

$$\frac{\partial \Sigma_{\rm H_2O}}{\partial t} + \frac{1}{R}\frac{\partial}{\partial R}\left[R\left(\Sigma_{\rm H_2O} u_R - \delta_R \frac{c_s^2}{\Omega}\Sigma \frac{\partial}{\partial R}\left(\frac{\Sigma_{\rm H_2O}}{\Sigma}\right)\right)\right] = -S_{\rm coll} \tag{6}$$

with $S_{\rm coll}$ the sink term resulting from collisions — both coagulation and shattering processes (contributing positively and negatively to it, respectively) —, and δ_R a dimensionless number (of order α) parameterizing turbulent diffusion. We neglect any gas-solid drift induced by gas drag (we shall return to this assumption in Section 4.2).

If coagulation and shattering can be ignored, it is straightforward to see that $\Sigma_{\rm H_2O} \propto \Sigma$ is a solution of the equation. This should remain a reasonable approximation for coagulation timescales longer than $t_{\rm vis}$. There is evidence suggesting that accretion was indeed quite inefficient/slow in the early solar system: age dating of chondrite components and studies of the thermal evolution of their parent bodies are consistent with accretion being a protracted process on a few-Ma timescale (e.g. Villeneuve *et al.* 2009; Grimm and McSween 1989; Kleine *et al.* 2008; Connelly *et al.* 2012) and the total mass of the current planetary system (see e.g. Hayashi 1981) is one order of magnitude lower than the nonvolatile content of disks at the end of the infall phase (e.g. Yang and Ciesla 2012) assuming a solar metallicity. We shall thus assume that accretion was inefficient and ignore its feedback on the dynamics of nebular water so that $\epsilon_{\rm H_2O} \equiv \Sigma_{\rm H_2O}/\Sigma$ can be considered constant (we shall return to this issue in Section 4).

2.3. Hydrogen isotopic composition of water

In this paper, we assume that the D/H ratio of water is dictated by isotopic exchange between originally isotopically heavy (comet-like) water and isotopically light hydrogen gas (e.g. Drouart *et al.* 1999; Mousis *et al.* 2000; Hersant *et al.*

[2] This is the evolution expected from the self-similar solution of the continuity equation for $\alpha c_s^2/\Omega \propto R$ (see e.g. Garaud 2007) as is the case here in the outer disk.

2001). To make the problem analytically tractable, we circumvent an accurate treatment of reaction kinetics by schematically distinguishing between two types of water: *cometary water* is water that has never experienced temperatures in excess of a "reaction temperature" $T_{\rm reac}$ during the classical T Tauri stage of the disk, and is assumed to retain a relatively heavy D/H ratio denoted $({\rm D/H})_h$; *equilibrated water*, on the other hand, is water that did experience temperatures above $T_{\rm reac}$ and therefore has a D/H ratio set to a fixed value $({\rm D/H})_l$ through isotopic exchange with hydrogen gas (a justification for this treatment based on reaction kinetics is provided in Appendix B). $T_{\rm reac}$, $({\rm D/H})_l$ and $({\rm D/H})_h$ are fixed parameters of the model and are assigned values of 500 K, 40×10^{-6} and 300×10^{-6} for them, respectively (see Appendix B). The value of 40×10^{-6} corresponds to the maximum D/H ratio that can be reached by water in equilibrium with molecular hydrogen. Indeed, although enrichment in D could be in principle higher at lower equilibration temperature, slow kinetics of the isotopic exchange reaction prevent this equilibrium from being actually attained below $T_{\rm reac}$.

We denote by $R_{\rm reac}$ the heliocentric distance where $T = T_{\rm reac}$, which is given by:

$$\begin{aligned} R_{\rm reac} &= \left(\frac{3\kappa m\dot{M}^2(GM_\odot)^{3/2}}{128\pi^2\sigma_{\rm SB}k_B\alpha T_{\rm reac}^5}\right)^{2/9} \\ &= 1\ {\rm AU}\dot{M}_{-8}^{4/9}\left(\frac{\kappa}{0.5\ {\rm m^2/kg}}\frac{10^{-3}}{\alpha}\right)^{2/9}\left(\frac{500\ {\rm K}}{T_{\rm reac}}\right)^{10/9} \end{aligned} \quad (7)$$

with $\dot{M}_{-8} \equiv \dot{M}/(10^{-8}\ {\rm M_\odot\cdot a^{-1}})$, in the viscous-dominated regime. The mass accretion rate where $R_{\rm reac}$ enters the irradiation-dominated regime (see equation (C.4)) is in our model:

$$\begin{aligned} \dot{M}_{\rm reac} &= \left(\frac{128\pi^2\sigma_{\rm SB}k_B\alpha(f_T T_0)^9}{3\kappa m\Omega_0^3 T_{\rm reac}^4}\right)^{1/2} \\ &= 4\times10^{-11}\ {\rm M_\odot.a^{-1}}\left(\frac{\alpha}{10^{-3}}\frac{0.5\ {\rm m^2/kg}}{\kappa}\right)^{1/2}\left(\frac{f_T}{0.5}\right)^{9/2} \\ &\quad \left(\frac{500\ {\rm K}}{T_{\rm reac}}\right)^2 \end{aligned} \quad (8)$$

which is a very low value (compared e.g. to mass accretion rates reported by Hartmann *et al.* 1998) so the disk is likely to have largely dissipated by that time. Moreover, it may be seen from equation (C.4) that then $R_{\rm reac} \lesssim 0.1$AU, most likely inside the inner edge of the disk. So certainly at that time the validity of our disk model has broken down. We will find it convenient to take the corresponding time $t_{\rm reac}$ as the final time in our calculation.

Outside $R_{\rm reac}$, the surface density of equilibrated water $\Sigma_{\rm H_2O,eq}$ is governed by the same equation as total water, i.e. equation (6) with $\Sigma_{\rm H_2O}$ replaced by $\Sigma_{\rm H_2O,eq}$. A stationary solution to this equation, expected to be attained by $t_{\rm vis}$, is given by (Clarke and Pringle 1988; Stevenson 1990, see also Appendix A)

$$\frac{\Sigma_{\rm H_2O,eq}}{\Sigma_{\rm H_2O}} = \left(\frac{R_{\rm reac}}{R}\right)^{3{\rm Sc}_R/2} \quad (9)$$

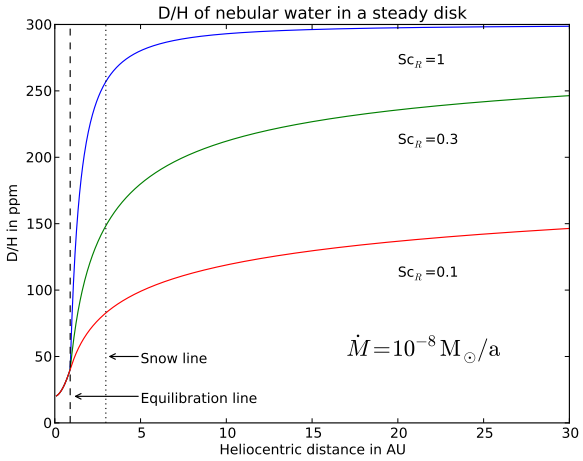

Figure 2: D/H ratio (expressed in parts per million (ppm)) of water as a function of heliocentric distance in a steady disk, for three values of the radial Schmidt number ${\rm Sc}_R$. In the "reaction zone", delimited by a vertical dashed line ("equilibration line"), equilibrium isotopic fractionation with hydrogen gas is assumed ; beyond, mixing with cometary water controls the D/H ratio (equation (11)). We have taken $\dot{M} = 10^{-8}$ M$_\odot$/a, $\alpha = 10^{-3}$, $\kappa = 0.5$ m^2/kg, $f_T = 0.5$. The smaller the ${\rm Sc}_R$, the more efficient radial mixing is. The position of the snow line (where water condenses) is indicated by a vertical dotted line: water is gaseous inside the snow line and solid outside.

where we have introduced the radial Schmidt number

$${\rm Sc}_R = \frac{\alpha}{\delta_R}. \quad (10)$$

We will henceforth adopt this solution. In other words, we assume that the radial distribution of equilibrated water undergoes a quasi-static evolution as the mass accretion rate (and thus $R_{\rm reac}$) decreases.

In this case, the D/H ratio of the total nebular water is given by[3]:

$$\left(\frac{\rm D}{\rm H}\right)(R,t) = \left(\frac{\rm D}{\rm H}\right)_h - \left(\left(\frac{\rm D}{\rm H}\right)_h - \left(\frac{\rm D}{\rm H}\right)_l\right)\left(\frac{R_{\rm reac}(t)}{R}\right)^{3{\rm Sc}_R/2}. \quad (11)$$

Thus, D/H is a monotonically increasing function both of heliocentric distance and time (as over time $\dot{M}$ and hence $R_{\rm reac}$ decrease). This is plotted in Fig. 2 and 3.

2.4. Accretion and delivery to Earth of water-bearing chondrites

At this point, we have wholly prescribed the isotopic and transport properties of nebular water in our model. We have yet to relate this nebular water to the D/H distribution of chondrites.

We first need to make a prescription for coagulation/shattering, which determines the rate at which water is incorporated in chondritic bodies. Similarly to Cassen (1996) (see also Ciesla and Cuzzi 2006; Weidenschilling 2004), we posit a collision term of the form

$$S_{\rm coll}(R,t) = \frac{\Sigma_{\rm H_2O}}{t_{\rm coag}(R)}\theta(R - R_{\rm cond}(t)), \quad (12)$$

[3] We use the fact that D/H$\ll 1$.

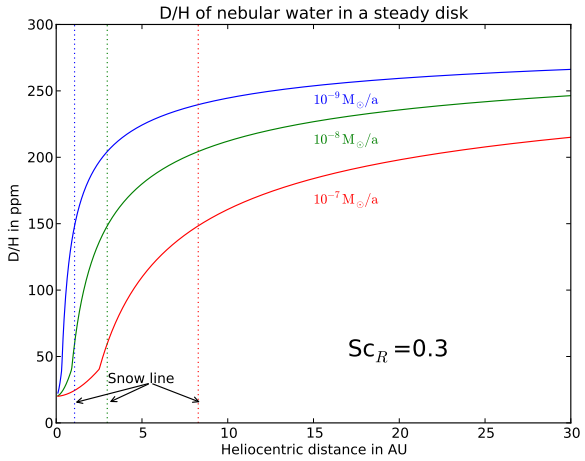

Figure 3: Same as Fig. 2 but for a fixed Sc$_R$=0.3 and with varying mass accretion rates.

with the coagulation timescale $t_{\rm coag}(R)$ taken to scale like the local orbital timescale (Ω^{-1}), θ the Heaviside function defined by

$$\theta(z) = \begin{cases} 0 \text{ if } z < 0 \\ 1 \text{ if } z \geq 0 \end{cases} \quad (13)$$

We thus consider that water is accreted solely as ice.

We finally need to prescribe the delivery of accreted material to the Earth as a function of the heliocentric distance of initial agglomeration. While this step encompasses a variety of processes such as drift of meter-sized boulders, orbital evolution of parent bodies and eventually ejected meteoroids, we will be content in assuming a *uniform* probability of delivery of material to Earth up to a maximum initial heliocentric distance $R_{\rm max}$. In other words, the distribution we are calculating will be representative of water ice accreted inside $R_{\rm max}$. If the asteroid main belt accreted *in situ*, $R_{\rm max}$ could be taken to correspond to its outer edge, near 3 AU. If, on the other hand, significant redistribution of planetesimals occurred, e.g. during the "Grand Tack" studied by Walsh *et al.* (2011), $R_{\rm max}$ could be considerably larger.

3. Results

Under the above hypotheses, meteoritic water, having been accreted from a range of heliocentric distances (between the snow line and $R_{\rm max}$) and at various times, will necessarily exhibit a range of D/H ratios and one can define a probability distribution function (PDF) for that quantity. The derivation and the expression of the PDF are presented in Appendix C and plots of it are shown in Fig. 4. It is notable that they are independent of α, t_0, $t_{\rm coag}(1\ {\rm AU})$ $\epsilon_{\rm H_2O}$ and κ and depend on f_T, $T_{\rm cond}$, $T_{\rm reac}$, $({\rm D/H})_h$, $({\rm D/H})_l$, $R_{\rm max}$ and Sc$_R$, of which only the latter two are considered free parameters.

Distributions exhibit a minimum cutoff value $({\rm D/H})_{\rm min,0}$ (see equation (C.8)). This minimum value of the distribution stems from the constraint that the accreted water be condensed, and

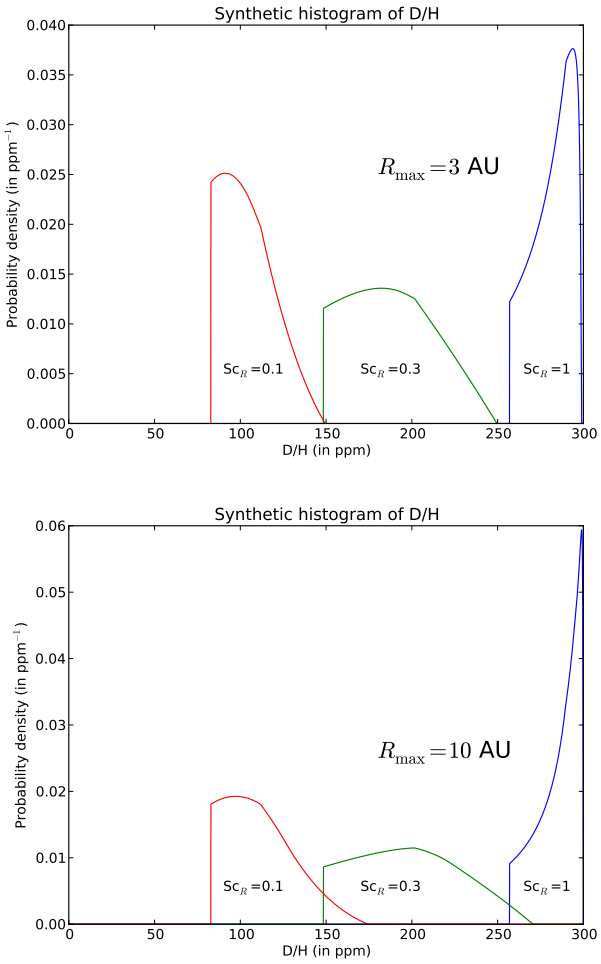

Figure 4: Probability distribution function of D/H calculated for different values of the radial Schmidt number Sc$_R$, assuming a maximum heliocentric distance of accretion $R_{\rm max}$ of 3 AU (Top) and 10 AU (Bottom). The lower the Sc$_R$ (that is, the larger the diffusivity), the more the PDF is peaked toward low values, while the larger the $R_{\rm max}$, the more the PDF is skewed toward heavy isotopic compositions.

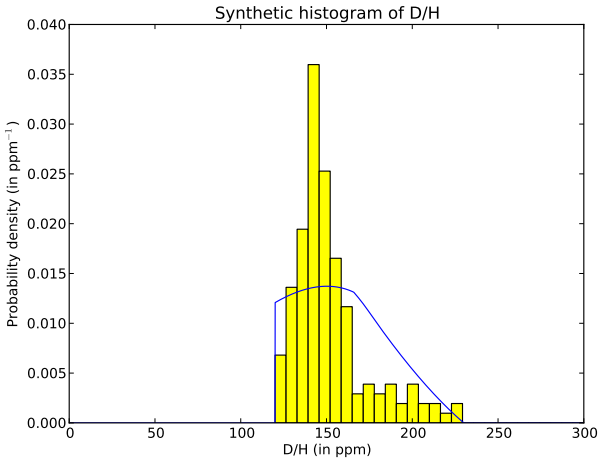

Figure 5: Probability distribution function of D/H values in bulk carbonaceous chondrites (CI, CO, CV, CM) compared to the theoretical PDF adjusted to fit the minimum and maximum of the distribution. The comparison is warranted only if isotopic exchange with organic matter on the parent body is negligible. Data from Kerridge (1985); Kolodny *et al.* (1980); Boato (1954); Robert and Epstein (1982); McNaughton *et al.* (1982); Yang and Epstein (1983); Pearson *et al.* (2001); Alexander *et al.* (2012b).

corresponds to the hydrogen isotopic composition of water at the snow line. It is thus governed by isotope exchange kinetics (which determines the composition and origin of equilibrated water) *and* radial transport to the snow line (which determines the proportion of equilibrated water there) alike. It is noteworthy that the D/H ratio at the snow line does not evolve with time (so long it is in the viscous-heating dominated temperature region), as it only depends on the ratio $T_{\rm cond}/T_{\rm reac}$ (see equation (C.5)).

As is apparent on each panel of Fig. 4, low values of $({\rm D/H})_{\rm min,0}$ are associated with efficient radial mixing (enabling a high proportion of equilibrated water at the snow line), that is, a small radial Schmidt number, through the relationship (using equation (C.8)):

$$ {\rm Sc}_R = \frac{3}{5} \frac{\ln\left(\frac{({\rm D/H})_h - ({\rm D/H})_l}{({\rm D/H})_h - ({\rm D/H})_{\rm min,0}}\right)}{\ln\left(\frac{T_{\rm reac}}{T_{\rm cond}}\right)} \qquad (14) $$

For our fiducial parameters, if we adopt $({\rm D/H})_{\rm min,0} = 120\times10^{-6}$ from the observed PDF of D/H in carbonaceous chondrites, we obtain ${\rm Sc}_R$=0.2.

A low value of ${\rm Sc}_R$ is also needed if one is to recover the positive skewness of the observed PDF (with a negative slope over most of the range of D/H values). Indeed, equation (C.3) indicates that the PDF has an overall dependence in $[({\rm D/H})_h - ({\rm D/H})]^{1/(3{\rm Sc}_R)-1}$, notwithstanding "second-order" modifications imposed by the constraint $R_{\rm cond} < R < R_{\rm max}$ and the changes in the temperature regime. This imposes an overall decreasing trend if ${\rm Sc}_R \lesssim 1/3$.[4] Efficient transport indeed means that the D/H ratio will be close to that at the snow line for a significant fraction of the outer disk, hence the dominance of this value in the PDF.

By comparing the two panels of Fig. 4, it is also apparent that the PDF is also more skewed toward higher D/H ratio if $R_{\rm max}$ increases, as is expected from the monotonic increase of D/H with increasing heliocentric distance in our model. The maximum value $({\rm D/H})_{\rm max,f}$ (see equation (C.11)) is related to $R_{\rm max}$ through the relationship (injecting equation (14) into equation (C.11)):

$$ R_{\rm max,AU} = \left(\frac{f_T T_0}{T_{\rm reac}}\right)^2 \exp\left(\frac{10}{9} \frac{\ln\left(\frac{T_{\rm reac}}{T_{\rm cond}}\right) \ln\left(\frac{({\rm D/H})_h - ({\rm D/H})_l}{({\rm D/H})_h - ({\rm D/H})_{\rm max,f}}\right)}{\ln\left(\frac{({\rm D/H})_h - ({\rm D/H})_l}{({\rm D/H})_h - ({\rm D/H})_{\rm min,0}}\right)}\right) \qquad (15) $$

If we adopt $({\rm D/H})_{\rm max,f} = 230\times10^{-6}$, one obtains $R_{\rm max} = 6$ AU. $R_{\rm max}$ as expressed above is however quite sensitive to the assumed parameters, and as such our calculation would not conclusively discriminate between *in situ* formation of the asteroid main belt and widespread redistribution (Walsh *et al.* 2011). Note that the evaluations of both ${\rm Sc}_R$ and $R_{\rm max}$ in equations (14) and (15) are independent of our prescriptions of accretion of solids or the functional form of $\dot{M}(t)$.

In Fig. 5, we have plotted the theoretical PDF with the ${\rm Sc}_R$ and $R_{\rm max}$ evaluated above (which by construction adjust the PDF to the minimum and maximum observed values and the histogram of the latter (observed) data). The shape of the observed PDF is reproduced qualitatively (though not quantitatively), with (i) a peak near the lower end of the distribution and (ii) a tail toward high D/H ratios. The peak corresponds to D/H ratios near the snow line, which dominate the distribution because accretion is most efficient there (because of shorter dynamical timescales and higher surface densities) than further from the Sun and also because efficient outward transport has almost homogenized the D/H ratios to the snow line value over an extensive region beyond it. The tail corresponds to water ice accreted some distance beyond the snow line, until the maximum heliocentric radius sampled.

However, the match is not quantitative, as the observed PDF is more peaked (around ${\rm D/H} = 150\times10^{-6}$) than the theoretical prediction. Certainly, the simplifications used in the model (e.g. constant α, prescription of delivery to Earth etc.) prevent it from yielding realistic PDFs and only allow a proof-of-concept use. We shall now discuss implications of these results as well as assess the limitations of our treatment.

4. Discussion

4.1. Implications

From the above results, it appears that the distribution of D/H ratios of carbonaceous chondrites can be accounted for in a scenario of isotopic exchange with hydrogen gas, with cometary D/H values prevailing at large heliocentric distances, under the condition that the radial Schmidt number ${\rm Sc}_R$ be small ($\lesssim 0.3$).

[4] Note that this inequality does not depend on the prescription we have adopted for $\dot{M}(t)$ but does depend on the power law for the irradiation-dominated temperature regime and that of the coagulation timescale: for $T \propto R^{-q}$ and $t_{\rm coag} \propto R^a$, the inequality becomes ${\rm Sc}_R \lesssim (2(a-q)-1)/3$ (going back to equation (C.1))

The peak value of the carbonaceous chondrite population would be essentially dictated by the isotopic composition of water near the snow line, where accretion of *condensed* water would be most efficient.

The low values inferred for Sc_R would be consistent with hydrodynamical turbulence (e.g. Prinn 1990; Dubrulle and Frisch 1991; Gail 2001) — e.g. the 0.176 value measured by Lathrop *et al.* (1992), although more experimental (and numerical) data would be desirable. It would not be consistent, however, with magnetohydrodynamic (MHD) turbulence (Johansen *et al.* 2006). MHD turbulence, mainly driven by the magnetorotational instability (MRI; Balbus and Hawley 1998), is widely believed to be the driver of transport in accretion disks. However, there must be a region in the disk, referred to as the *dead zone*, which is too cold and dense for the MRI to operate (Gammie 1996). In the dead zone, turbulence should be of low intensity and hydrodynamical in nature. Thus our results are consistent with the idea that the planetesimals sampled by chondrites formed in this purported dead zone. In fact, ionization fraction calculations have shown that the dead zone would encompass the whole planet-forming region (from ~0.1 to a few 10s of AU, e.g. Bai and Goodman 2009) and indeed a dead zone would be a most favorable environment for planet formation (Terquem 2008). Moreover the existence of a dead zone has been found to enable the preservation of chondrite components for a few Ma in the disk (Jacquet *et al.* 2011).

The low value of Sc_R would not only have enhanced outward transport of equilibrated water, but also that of higher-temperature components as well (see also Bockelée-Morvan *et al.* 2002). This could account for the high-temperature minerals, including calcium-aluminum-rich inclusions (CAIs) and chondrule fragments identified in comet Wild 2 samples (Zolensky *et al.* 2006; Bridges *et al.* 2012) and also the relatively high abundances of CAIs in carbonaceous chondrites (see Jacquet *et al.* 2012).

If mixing was as efficient as inferred above, the D/H ratio could have been significantly lower than $(\mathrm{D/H})_h$ even at a few tens of AUs, depending on time (see Fig. 2). Thus, comets may have formed with D/H ratios lower than $(\mathrm{D/H})_h$ (the limit at large heliocentric distances), which would account for the emerging range in measured D/H ratios of cometary water (Hartogh *et al.* 2011; Bockelée-Morvan *et al.* 2012), consistent with the idea of an asteroid-comet continuum (Gounelle *et al.* 2008; Briani *et al.* 2011). Even the 300×10^{-6} value adopted for $(\mathrm{D/H})_h$ on the basis of measurements of known comets could then actually be a lower bound of its real value.

4.2. Modeling caveats

Of course the validity of the conclusions of this study can only be as good as that of its underlying assumptions.

First, the quasi-static approximation we have used requires, as we recall from Section 2.1, that the viscous timescale $t_{\mathrm{vis}}(R)$ be short relative to the time of chondrite accretion and that of evolution of the mass accretion rate. In a dead zone, whose existence we have inferred above, α would likely be small, around 10^{-4} (e.g. Fleming and Stone 2003; Ilgner and Nelson 2008; Oishi and Mac Low 2009; Turner *et al.* 2010), so that t_{vis} would

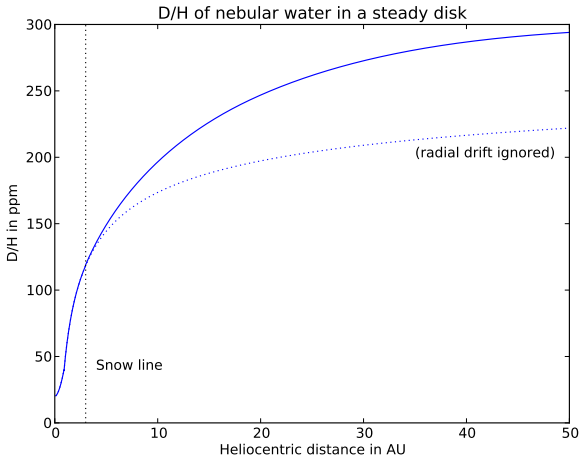

Figure 6: The D/H ratio as a function of heliocentric distance of accretion, for the radial Schmidt number inferred from this study (0.2) at a fiducial time where the snow line lies at 3 AU from the Sun. We have taken $\kappa = 0.5\,\mathrm{m}^2/\mathrm{kg}$ and $\alpha = 10^{-4}$ (as appropriate in a dead zone). To realistically extrapolate to the comet-forming regions, we have here taken into account the effect of radial drift by considering millimeter-sized grains ($\rho_s a = 1\,\mathrm{kg/m}^2$; see Appendix A). The D/H curve without this effect is also shown for comparison (dotted line).

be longer than our nominal evaluation in equation (3), but at $R = 3$ AU, it would be ~1 Ma, still shorter than the accretion time of chondrites after the start of the solar system (~1-5 Ma, see e.g. Villeneuve *et al.* (2009); Connelly *et al.* (2012)). Admittedly, the timescale constraint would be quite marginally satisfied, so that, conceivably, future re-examination of this problem in time-dependent simulations of disks with dead zones, with self-consistently evaluated α (see e.g. Zhu *et al.* (2010)), could unveil new interesting effects. Nonetheless, this would not affect our conclusion that MRI-turbulent disk models, with higher α—hence largely satisfying the timescale constraint—and Sc_R, cannot reproduce the D/H ratio of chondrites and our inference of the presence of dead zone thus appears robust in this respect.

Our steady-state disk model neglects photoevaporation during the bulk of the disk's lifetime. However, if, as argued by Desch (2007), the disk was subject to intense photoevaporation from the outset, the net gas flow could have been *outward*, and equilibrated water would have reached the snow line almost undiluted; i.e. water at the snow line would have a D/H ratio close to $(\mathrm{D/H})_l \approx 40 \times 10^{-6}$. If such isotopically light *bulk* preaccretionary water compositions were to be found in the future, this would be a possibility worth investigating ; however, to date, such isotopic compositions have not been measured.

In this work, nebular water has been assumed to be dynamically coupled to the gas. Depending on the fragmentation and the bouncing barriers (e.g. Zsom *et al.* 2010; Birnstiel *et al.* 2012), it is however conceivable that ice-bearing particles grow to millimeter-size and beyond so that drift due to gas drag would be significant (see equation (A.5)) before they are incorporated in planetesimals. This would likely lead to significant enhancements of water abundance inside and at the snow line, and depletions further outwards (e.g. Cuzzi and Zahnle 2004;

Ciesla and Cuzzi 2006). From equation (A.8) derived in Appendix A, it can be seen that the fraction of equilibrated water would be lower, and thus D/H higher, than under our tight coupling calculation, because of increased import of "cometary water". One example of this effect is shown in Fig. 6 using the parameters inferred from this study. While the effect might be limited for the carbonaceous chondrites which we have focused on—for which Jacquet *et al.* (2012) inferred that millimeter-sized components were not significantly drifting—, it would certainly accelerate the convergence of the D/H ratio toward its asymptotic value in the comet-forming region (for $S_R > 1$, see Appendix A). This could account for the apparent carbonaceous chondrite/comet hydrogen isotopic dichotomy, in the sense that relatively little material with intermediate composition would then exist (but does exist, as emphasized at the end of Section 4.1). However, regardless of the actual quantitative importance of radial drift, it must be noted that inasmuch as nebular water *inside* the snow line would be in vapor state — even meter-sized solids would lose their water by vaporization before they can travel much inward of it (Cuzzi and Zahnle 2004) — and thus continue to be tightly coupled to the gas, the transport of equilibrated water until the snow line would be unchanged (see equation A.8) — save for some transition period preceding establishment of the quasistatic regime. Therefore, our estimate of Sc_R from the minimum D/H of the distribution (established at the snow line) would be unaffected and is thus robust in this regard too.

We have also argued that accretion was inefficient, allowing us to ignore feedback on the transport of nebular water. If this approximation were not to hold, rapid accretion of planetesimals at the snow line could progressively deplete the inner solar system in water (e.g. Ciesla and Cuzzi 2006). Although, again, this would likely not affect the D/H ratio at the snow line, the effects on the shape of the PDF have yet to be determined by dedicated numerical simulations including both coagulation and shattering (see Yang *et al.* 2012).

4.3. On the interpretation of D/H chondrite data

In this work, we have compared our PDF of the isotopic composition of water to bulk chondrite compositions (see Fig. 5), and, in doing so, implicitly assumed that the latter reflected the composition of pre-accretionary water now locked in hydrated silicates. However, hydrated silicates are not the only contributors to the hydrogen budget of carbonaceous chondrites, as the latter also contain organic matter. The rationale for making this identification nonetheless is that inasmuch organic matter does not account for more than 10 % of the hydrogen, at their *presently measured* D/H ratios (mostly $\lesssim 400 \times 10^{-6}$—still excluding CR chondrites—; Alexander *et al.* (2010)), the incurred shifts to the isotopic composition would be small ($\lesssim 20 \times 10^{-6}$; Robert (2006)) compared to the observed range of D/H ratios. However, this ignores the possibility of isotopic exchange between organic matter and water on the parent body, in which case the organic matter could have been much more D-rich initially than presently measured. In fact, Alexander *et al.* (2012b) showed that the D/H ratio of bulk carbonaceous chondrites correlated positively with the C/H ratio, and interpreting this as a mixing trend, extrapolated an initial D/H ratio for organic matter comparable to that of CR chondrites ($\approx 700\times10^{-6}$), and consequently, a lighter isotopic composition for pre-accretionary water, e.g. $(86.5 \pm 3.5) \times 10^{-6}$ for CM chondrites[5]. In that case, while (direct) comparison of the theoretical PDF with the histogram plotted in Fig. 5 would no longer make sense, $(\mathrm{D/H})_{\mathrm{min},0}$ would be constrained to be lower than this latter value, and our formalism would thus constrain Sc_R to be $\lesssim 0.1$ (see equation (14)), that is, a yet more efficient radial diffusion would be indicated.

It must be cautioned, though, that *in situ* observations of CI, CM and CR chondrite matrices have revealed little evidence of isotopic exchange between the isotopically heterogeneous organic matter and the intermixed hydrous minerals (Remusat *et al.* 2010) and organic matter in the least aqueously altered CM chondrite Paris has an hydrogen isotopic signature indistinguishable of that of the other CM (Remusat *et al.* 2011). One possible explanation for the D/H - C/H correlation of Alexander *et al.* (2012b) could be that the cometary water endmember was somehow coupled to D-rich organic matter in the disk, consistent with the high carbon contents of cometary grains (e.g. Wozniakiewicz *et al.* 2012). In that case, the mixing trend would not actually extrapolate to the composition of the organic matter but to that of the resulting *composite* (water+organics) C- and D-rich endmember. In this picture, the hydrogen isotopic signatures of organic matter and hydrated silicates could be actually largely pristine, as inferred by Remusat *et al.* (2010). Whatever that may be, and whether D/H ratios of bulk carbonaceous chondrites truly reflect the D/H ratios of preaccretionary water or only provide *upper* limits, we stress that low Schmidt numbers are robustly required in the framework of our formalism.

While the present work has mainly focused on carbonaceous chondrites, it is noteworthy that non-carbonaceous chondrites are generally richer in deuterium than the former (e.g. Robert 2006; Alexander *et al.* 2012b)[6]. As the D/H ratio of nebular water increases with time in our scenario, this could imply that they accreted *later* than the former, as suggested by Jacquet *et al.* (2012) based on the modeled redistribution of chondrite components in the disk. Conceivably, radial drift, as alluded to in the preceding subsection, which would be most pronounced as the coupling of the grains with the less dense gas would be looser then, might have contributed to significant enhancements of the D/H ratios for them. In fact, Jacquet *et al.* (2012) specifically inferred that millimeter-size components were significantly drifting for these chondrites, and from equation (A.8), the nebular water should be isotopically close to cometary values, which appears to be the case for clays from unequilibrated ordinary chondrites (e.g. Robert 2006; Alexander *et al.* 2012b).

[5] This would incidentally explain some low-D/H point measurements in LL3 chondrites (Deloule *et al.* 1998).

[6] Alexander *et al.* (2012a) suggest that the high D/H ratios of these meteorites could be due to oxidation of metallic iron by water producing isotopically light hydrogen gas escaping from the system. However, while this may have affected metamorphosed chondrites (Alexander *et al.* 2010; McCanta *et al.* 2008), the most unequilibrated ordinary chondrites also show these high values, with considerable heterogeneity consistent with the pristinity of this signature (Piani 2012).

A later formation of the non-carbonaceous chondrites would avoid the alternative possibility of an accretion *further* from the Sun than carbonaceous chondrites, which would run counter to the observed distribution of asteroid classes (e.g. Burbine *et al.* 2008). A later formation time could also account for the high D/H values of CR chondrites too—consistent with their young chondrule Al-Mg ages (Kita and Ushikubo 2012)—, which could mark an intermediate status between the other carbonaceous and the non-carbonaceous chondrites—along with their rather low refractory inclusions abundance, their limited refractory element enrichment relative to Mg, and their relatively heavy oxygen isotopic composition (Scott and Krot 2003).

5. Summary

We have considered a simplified analytic model for water transport and isotopic evolution in an evolving disk based on the following main assumptions:

(i) The regions of interest of the disk are approximated by a stationary model, with a constant turbulence parameter α.

(ii) Accretion is inefficient and does not significantly affect the transport of nebular water.

(iii) Water far from the Sun is assumed to have the same D/H ratio as cometary water, and any batch of water having experienced temperatures above a "reaction temperature" $T_{\rm reac}$ has had its D/H reset to a fixed value $({\rm D/H})_l$.

(iv) Accretion is modeled by a coagulation timescale scaling with the orbital period and water is incorporated as ice only. A uniform probability of delivery to Earth is applied to agglomeration locations up to a maximum heliocentric distance $R_{\rm max}$.

In this model, the D/H ratio of water is an increasing function of time and heliocentric distance. After integration over time, the probability distribution function (PDF) of the D/H ratio in accreted water is found to depend essentially on $R_{\rm max}$ and (most sensitively) on the radial Schmidt number ${\rm Sc}_R \equiv \alpha/\delta_R$ with δ_R parameterizing the diffusivity. The minimum cutoff of the PDF is determined by isotopic composition of water at the snow line, while the isotopically heavy tail is dictated by $R_{\rm max}$.

It appears that the model is able to broadly account for the observed PDF in carbonaceous chondrites if low values of ${\rm Sc}_R$ (around 0.1-0.3)—i.e. efficient outward diffusion—are assumed in order to reproduce the low D/H values of most chondrites and the positive skewness of the observed distribution. This would be most consistent with hydrodynamical turbulence as expected to prevail in the dead zone of the protoplanetary disk. Efficient outward diffusion would also have enabled the transport of high-temperature minerals to comets. The high D/H ratios in CR chondrites and non-carbonaceous chondrites could indicate an accretion later than most carbonaceous chondrites.

The effects of radial drift and higher accretion efficiencies on the transport of water and its hydrogen isotopic composition have yet to be investigated.

Acknowledgement

We thank the two anonymous referees for their reviews which improved the clarity of the paper in particular as to the effects of radial drift and the transition to cometary isotopic signatures.

Appendix A. Diffusion of equilibrated water in disks

In this appendix, we calculate the steady-state profile of nebular water concentration and its equilibrated fraction. To allow discussion of the tight coupling assumption in Section 4, we take into account the finite size of ice-bearing particles beyond the snow line, and thence the effects of gas drag, so that their velocity becomes, ignoring any feedback of the solids on the gas (e.g. Birnstiel *et al.* 2010):

$$v_R = \frac{1}{1+{\rm St}^2}\left(-\frac{3}{\Sigma R^{1/2}}\frac{\partial}{\partial R}\left(R^{1/2}\Sigma\nu\right)+\frac{\tau}{\rho}\frac{\partial P}{\partial R}\right), \quad (A.1)$$

with $\nu = \alpha c_s^2/\Omega$ the turbulent viscosity, τ the gas drag stopping time, ${\rm St} \equiv \Omega\tau$ the Stokes number, and P and ρ the gas pressure and density, respectively.

In steady state, the mass accretion rate of nebular water

$$\dot{M}_{\rm H_2O} = 2\pi R\left(-\Sigma_{\rm H_2O}v_R + D_R\Sigma\frac{\partial}{\partial R}\left(\frac{\Sigma_{\rm H_2O}}{\Sigma}\right)\right), \quad (A.2)$$

is constant. We have introduced the diffusion coefficient modified by finite particle size as (Youdin and Lithwick 2007)

$$D_R = \frac{\delta_R c_s^2/\Omega}{1+{\rm St}^2}. \quad (A.3)$$

Equation (A.2) may be viewed as a first-order ordinary differential equation in $\Sigma_{\rm H_2O}/\Sigma$. It is noteworthy that the corresponding homogeneous equation is the equation governing the transport of equilibrated water, since its concentration vanishes at infinity, so that:

$$\frac{\Sigma_{\rm H_2O,eq}}{\Sigma} \propto \exp\left(\int^R \frac{v_R}{D_R}{\rm d}R'\right) \propto \frac{\exp\left(\int^R S_R\frac{\partial \ln P}{\partial R}{\rm d}R'\right)}{\left(\Sigma\nu R^{1/2}\right)^{3{\rm Sc}_R}} \quad (A.4)$$

where the second proportionality relationship assumes that ${\rm Sc}_R$ is radially constant and we have coined $S_R = {\rm St}/\delta_R$ which is a measure of gas-grain decoupling (Jacquet *et al.* 2012). In the Epstein drag regime, for spherical grains of density ρ_s and radius a (averaged over the size distribution), we have:

$$\begin{aligned} S_R = \frac{\pi}{2}\frac{\rho_s a}{\Sigma\delta_R} &= \frac{3\pi^2{\rm Sc}_R}{2}\frac{\rho_s a c_s^2}{\dot{M}\Omega} \\ &= 0.1\frac{{\rm Sc}_R R_{\rm AU}^{3/2}}{\dot{M}_{-8}}\left(\frac{\rho_s a}{1\,{\rm kg/m^2}}\right)\left(\frac{T}{300\,{\rm K}}\right), \end{aligned} \quad (A.5)$$

where the last two equations pertain to a steady disk as assumed in the main text. Note that the normalizing value $\rho_s a = 1\,{\rm kg/m^2}$ corresponds to millimeter-sized grains (the typical size of non-matrix chondrite components).

By requiring that Σ_{H_2O}/Σ does not diverge at the disk's inner edge (whose heliocentric distance we denote by R_{in}, taken to be zero in the main text), equation (A.2) may be then integrated as:

$$\frac{\Sigma_{H_2O}}{\Sigma} = \exp\left(\int_{R_{in}}^{R} \frac{v_R}{D_R} dR'\right) \int_{R_{in}}^{R} \exp\left(-\int_{R_{in}}^{R'} \frac{v_R}{D_R} dR''\right) \frac{\dot{M}_{H_2O} dR'}{2\pi R' \Sigma D_R} \quad (A.6)$$

For $S_R \ll 1$ (in particular inside the snow line where $S_R = 0$), this is a constant , and for $S_R \gg 1 \gg St$, it falls off as $1/S_R$. Then, the fraction of equilibrated water is:

$$\frac{\Sigma_{H_2O,eq}}{\Sigma_{H_2O}} \propto \left[\int_{R_{in}}^{R} \exp\left(-\int_{R_{in}}^{R'} \frac{v_R}{D_R} dR''\right) \frac{dR'}{R' \Sigma D_R}\right]^{-1} \quad (A.7)$$

Enforcing that the left-hand-side be unity at $R = R_{reac}$, this becomes:

$$\frac{\Sigma_{H_2O,eq}}{\Sigma_{H_2O}} = \frac{2}{3Sc_R} \left(\sqrt{R_{reac}} - \sqrt{R_{in}}\right)^{3Sc_R} \left[\int_{R_{in}}^{R} \left(\sqrt{R'} - \sqrt{R_{in}}\right)^{3Sc_R - 1} \exp\left(-\int_{R_{reac}}^{R'} S_R \frac{\partial \ln P}{\partial R} dR''\right) \left(1 + St^2\right) \frac{dR'}{\sqrt{R'}}\right]^{-1} \quad (A.8)$$

For $S_R \ll 1$, this amounts to equation (9) for $R_{in} \ll R_{reac} < R$.

Appendix B. Kinetics of water-hydrogen isotopic exchange

Ignoring transport, and given that $D/H \ll 1$ and $H_2O/H_2 \ll 1$, the equation governing the evolution of D/H of water may be written as (Lécluse and Robert 1994):

$$\frac{d}{dt}\left(\frac{D}{H}\right) = k^-(T) n_{H_2} \left(\left(\frac{D}{H}\right)_{eq}(T) - \left(\frac{D}{H}\right)\right) \quad (B.1)$$

with n_{H_2} the number density of hydrogen molecules, $(D/H)_{eq}$ the equilibrium values (see e.g. Richet *et al.* 1977) and the rate constant

$$k^-(T) = 2 \times 10^{-28} \exp\left(-\frac{5170\ K}{T}\right) m^3/s. \quad (B.2)$$

Given that, in our steady-state model, the midplane number density can be expressed as a function of temperature (assumed to be vertically constant) as

$$n_{H_2} = \frac{\Sigma\Omega}{\sqrt{2\pi} m c_s} = \frac{16}{9}\left(\frac{3}{\dot{M}\alpha}\right)^{1/3} \left(\frac{2T^{11}}{\pi k_B^5 m}\right)^{1/6} \left(\frac{\sigma_{SB}}{\kappa}\right)^{2/3} \quad (B.3)$$

the characteristic equilibration timescale resulting from equation (B.1) is:

$$t_{eq} \equiv \frac{1}{k^-(T) n_{H_2}} = 0.1\ Ma \frac{\exp\left(\frac{5170\ K}{T}\right)}{T_K^{11/6}} \left(\frac{\alpha \dot{M}_{-8}}{10^{-3}}\right)^{1/3} \left(\frac{\kappa}{0.5\ m^2/kg}\right)^{2/3} \quad (B.4)$$

This is a sharply decreasing function of temperature. While, at high temperature, t_{eq} is short compared to the transport timescale t_{vis} so that water vapor and hydrogen gas can be considered in equilibrium, at lower temperature (at larger heliocentric distances), t_{eq} becomes long compared to t_{vis} and isotopic exchange is essentially quenched. The temperature T_{reac} marking the transition between the two regimes can be determined by setting:

$$t_{eq}(T_{reac}) \equiv t_{vis}(T_{reac}). \quad (B.5)$$

Water originating from inside R_{reac} ("equilibrated water") will then essentially have the isotopic composition it had when it last equilibrated with hydrogen gas, i.e. at $T = T_{reac}$, that is, its D/H ratio will be $(D/H)_l \equiv (D/H)_{eq}(T_{reac})$.

Numerically, equation (B.5) can be expressed as:

$$\frac{\exp\left(\frac{5170\ K}{T_{reac}}\right)}{T_{reac,K}^{5/18}} = \frac{5 \times 10^3}{\dot{M}_{-8}^{1/9}} \left(\frac{10^{-3}}{\alpha}\right)^{13/9} \left(\frac{0.5\ m^2/kg}{\kappa}\right)^{5/9}. \quad (B.6)$$

The left-hand-side being a sharply decreasing function of T_{reac}, the sensitivity on $\dot{M}$ is completely negligible and that on α is also fairly weak. We shall thus adopt the solution of this equation for $\alpha = 10^{-3}$, $\dot{M} = 10^{-8}\ M_\odot/a$, $\kappa = 0.5\ m^2/kg$, which is $T_{reac} = 500\ K$. Adopting a protosolar D/H ratio (for the H_2 gas) of $(20 \pm 3.5) \times 10^{-6}$ (Geiss and Gloeckler 2003), the fractionation factor given by Richet *et al.* (1977) yields $(D/H)_l = 40 \times 10^{-6}$.

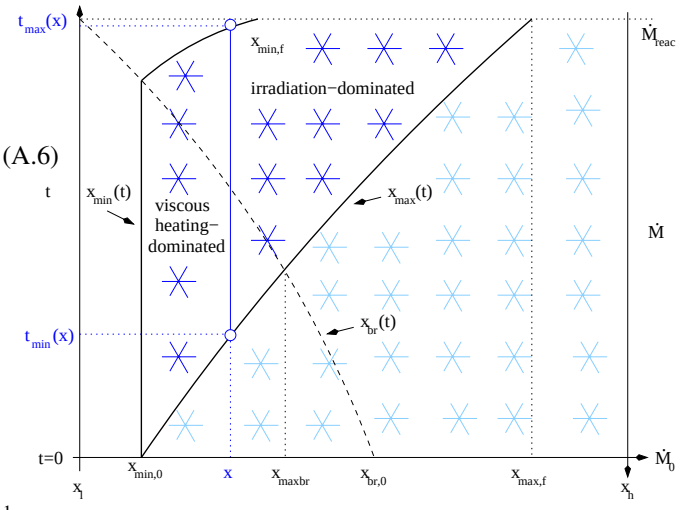

Figure C.7: A schematic diagram to help visualize the calculation and the different quantities involved. The abscissa is the D/H ratio (x) and the ordinate is the time t, or, correspondingly, the mass accretion rate $\dot{M}$. The snowflakes mark the domain where water is condensed and those colored in deep blue mark water ice inside heliocentric distance R_{max}, which contributes to the PDF. Their area is bounded by the thick black curves (x_{min} and x_{max}), while the dashed line marks the boundary between the viscous-heating and irradiation-dominated regimes (for the location corresponding having the D/H value of x at time t). With the passage of time, the average D/H ratio of water increases. The blue line represents the time interval of integration on the right-hand-side of equation (C.3) for a given value of x.

Appendix C. Calculation of the PDF of D/H

In this appendix, we detail the calculation of the PDF of the D/H ratio of meteoritic water. We will here denote D/H by x for the sake of legibility of the equations.

With the model set up in Section 2, the mass of meteoritic water with D/H ratio between x and $x + \mathrm{d}x$ is

$$\int_0^{t_{\rm reac}} S_{\rm coll}(R(x,t),t) 2\pi R(x,t) \frac{\partial R}{\partial x}_{|t} \mathrm{d}x \theta(R_{\rm max} - R(x,t)) \mathrm{d}t \propto f(x)\mathrm{d}x \quad \text{(C.1)}$$

where $f(x)$ is the normalized probability density function of bulk chondrites in terms of D/H ratio. $t = 0$ is taken to correspond to the time where $R_{\rm cond} = R_{\rm max}$, i.e. the earliest possible time where water can condense and be accreted inside $R_{\rm max}$, corresponding to the mass accretion rate

$$\begin{aligned} \dot{M}_0 &= \left(\frac{128\pi^2\sigma_{\rm SB}k_B\alpha T_{\rm cond}^5}{3\kappa m\Omega(R_{\rm max})^3}\right)^{1/2} \\ &= 1.5\times10^{-7}\ \mathrm{M_\odot.a^{-1}} \left(\frac{\alpha}{10^{-3}}\frac{0.5\ \mathrm{m^2/kg}}{\kappa}\right)^{1/2} \\ &\quad \left(\frac{T_{\rm cond}}{170\ \mathrm{K}}\right)^{5/2}\left(\frac{R_{\rm max}}{10\ \mathrm{AU}}\right)^{9/4} \end{aligned} \quad \text{(C.2)}$$

Using the assumed constancies of $\epsilon_{\rm H_2O}$, $\Omega t_{\rm coag}(R)$, α, Sc_R and using equation (2), we have:

$$\begin{aligned} f(x) &\propto \int_0^{t_{\rm reac}} \frac{\dot{M}(t)}{R_{\rm reac}(t)T(R(x,t),t)}(x_h - x)^{2/(3\mathrm{Sc}_R)-1} \\ &\quad \theta(R_{\rm max} - R(x,t))\theta(R(x,t) - R_{\rm cond}(t))\mathrm{d}t \\ &\propto (x_h - x)^{1/(3\mathrm{Sc}_R)-1}\int_{t_{\rm min}(x)}^{t_{\rm max}(x)} \left(\frac{\dot{M}(t)}{\dot{M}_0}\right)^{7/9} \\ &\quad \min\left(\left(\frac{\dot{M}_{\rm br}(x)}{\dot{M}(t)}\right)^{2/9}, 1\right)\mathrm{d}t \end{aligned} \quad \text{(C.3)}$$

with $t_{\rm min}(x)$ and $t_{\rm max}(x)$ determined by the conditions $R < R_{\rm max}$ and $R > R_{\rm cond}$, respectively, $\dot{M}_{\rm br}(x)$ the mass accretion rate for which $x(R_{\rm br}) = x$, where $R_{\rm br}$ is defined as the heliocentric distance of the transition between the viscous-heating- and the irradiation-dominated regimes and is given by (see equation (5)):

$$\begin{aligned} R_{\rm br,AU} &= \left(\frac{3}{128\pi^2}\frac{\kappa m}{\sigma_{\rm SB}k_B\alpha}\frac{\dot{M}^2\Omega_0^3}{(f_T T_0)^5}\right)^{1/2} \\ &= 3\,\frac{\dot{M}_{-8}}{f_T^{5/2}}\left(\frac{\kappa}{0.5\ \mathrm{m^2/kg}}\frac{10^{-3}}{\alpha}\right)^{1/2}. \end{aligned} \quad \text{(C.4)}$$

with $\Omega_0 \equiv \Omega(1\ \mathrm{AU})$. The "min(...)" factor in equation (C.3) is unity when $R(x,t)$ is in the irradiation-dominated regime.

Before proceeding to the result, we coin a few additional notations and then proceed to the integration. Fig. C.7 may help the reader to visualize the situation in the D/H - time space.

For a given mass accretion rate, the minimum and maximum value of D/H dictated by the conditions $R_{\rm cond} \le R \le R_{\rm max}$ are:

$$x_{\rm min}(\dot{M}) = \begin{cases} x_h - (x_h - x_l)\left(\frac{T_{\rm cond}}{T_{\rm reac}}\right)^{5\mathrm{Sc}_R/3} & \text{if } T_{\rm br} \le T_{\rm cond} \\ x_h - (x_h - x_l)\left(\left(\frac{T_{\rm cond}}{f_T T_0}\right)^3\left(\frac{3\kappa m\dot{M}^2\Omega_0^3}{128\pi^2\sigma_{\rm SB}k_B\alpha T_{\rm reac}^5}\right)^{1/3}\right)^{\mathrm{Sc}_R} & \\ \qquad \text{if } T_{\rm cond} < T_{\rm br} < T_{\rm reac} & \\ x_h - (x_h - x_l)\left(\frac{T_{\rm cond}}{T_{\rm reac}}\right)^{3\mathrm{Sc}_R} & \text{if } T_{\rm br} \ge T_{\rm reac} \end{cases} \quad \text{(C.5)}$$

and

$$x_{\rm max}(\dot{M}) = x_h - (x_h - x_l)\left(\frac{R_{\rm reac}(\dot{M})}{R_{\rm max}}\right)^{3\mathrm{Sc}_R/2} \quad \text{(C.6)}$$

The D/H ratio at $R = R_{\rm br}$ (for $\dot{M} \ge \dot{M}_{\rm reac}$) is:

$$x_{\rm br}(\dot{M}) = x_h - (x_h - x_l)\left(\frac{128\pi^2\sigma_{\rm SB}k_B\alpha(f_T T_0)^9}{3\kappa m\dot{M}^2\Omega_0^3 T_{\rm reac}^4}\right)^{5\mathrm{Sc}_R/12} \quad \text{(C.7)}$$

To all these, a "0" subscript will be added if evaluated for $\dot{M} = \dot{M}_0$ and "f" for $\dot{M} = \dot{M}_{\rm reac}$. Hence,

$$x_{\rm min,0} = x_{\rm max,0} = x_h - (x_h - x_l)\left(\frac{T_{\rm cond}}{T_{\rm reac}}\right)^{5\mathrm{Sc}_R/3} \quad \text{(C.8)}$$

$$x_{\rm br,0} = x_h - (x_h - x_l)\left(\frac{T_{\rm irr}(R_{\rm max})^9}{T_{\rm reac}^4 T_{\rm cond}^5}\right)^{5\mathrm{Sc}_R/12} \quad \text{(C.9)}$$

$$x_{\rm min,f} = x_h - (x_h - x_l)\left(\frac{T_{\rm cond}}{T_{\rm reac}}\right)^{3\mathrm{Sc}_R} \quad \text{(C.10)}$$

$$x_{\rm max,f} = x_h - (x_h - x_l)\left(\frac{T_{\rm irr}(R_{\rm max})}{T_{\rm reac}}\right)^{3\mathrm{Sc}_R} \quad \text{(C.11)}$$

where $T_{\rm irr}(R_{\rm max}) \equiv f_T T_0 R_{\rm max,AU}^{-1/2}$ is the irradiation temperature at heliocentric distance $R_{\rm max}$.

We will also need the D/H ratio when $R_{\rm br} = R_{\rm max}$, which is given by:

$$x_{\rm maxbr} = x_h - (x_h - x_l)\left(\frac{T_{\rm irr}(R_{\rm max})}{T_{\rm reac}}\right)^{5\mathrm{Sc}_R/3} \quad \text{(C.12)}$$

and the ratio $\dot{M}_{\rm reac}/\dot{M}_0$ between the final and the starting mass accretion rate:

$$\frac{\dot{M}_{\rm reac}}{\dot{M}_0} = \left(\frac{T_{\rm irr}(R_{\rm max})^9}{T_{\rm reac}^4 T_{\rm cond}^5}\right)^{1/2} \quad \text{(C.13)}$$

With all these notations, we can express the result of the integration in equation (C.3) as:

$$\begin{aligned} f(x) = C(x_h - x)^{1/(3\mathrm{Sc}_R)-1}\Bigg(2\left(\frac{x_h - x_{\rm br,0}}{x_h - x}\right)^{2/(15\mathrm{Sc}_R)} \\ -\frac{T_{\rm irr}(R_{\rm max})}{T_{\rm reac}^{13/18}T_{\rm cond}^{5/18}}\left(\frac{x_h - x_l}{x_h - x}\right)^{13/(30\mathrm{Sc}_R)} - \left(\frac{\dot{M}_{\rm reac}}{\dot{M}_0}\right)^{1/9} S(x)\Bigg), \end{aligned} \quad \text{(C.14)}$$

for $x_{\rm min,0} \le x \le x_{\rm maxbr}$, and

$$\begin{aligned} f(x) = C(x_h - x)^{1/(3\mathrm{Sc}_R)-1}\Bigg(\left(\frac{x_h - x}{x_h - x_{\rm min,0}}\right)^{1/(6\mathrm{Sc}_R)} \\ -\left(\frac{\dot{M}_{\rm reac}}{\dot{M}_0}\right)^{1/9} S(x)\Bigg) \end{aligned} \quad \text{(C.15)}$$

for $x_{\rm maxbr} \le x \le x_{\rm max,f}$.

Here, C is a normalization factor given by

$$C = \left[\mathrm{Sc}_R (x_h - x_l)^{1/(3\mathrm{Sc}_R)} \left(12 \frac{T_{\rm irr}(R_{\rm max})^{1/2} T_{\rm cond}^{1/18}}{T_{\rm reac}^{5/9}} - 18 \frac{T_{\rm irr}(R_{\rm max})^{5/6}}{T_{\rm reac}^{5/9} T_{\rm cond}^{5/18}} \right.\right.$$
$$\left.\left. + 10 \frac{T_{\rm irr}(R_{\rm max})}{T_{\rm cond}^{4/9} T_{\rm reac}^{5/9}} + \frac{T_{\rm irr}(R_{\rm max})^{3/2}}{T_{\rm cond}^{5/18} T_{\rm reac}^{11/9}} - \frac{T_{\rm irr}(R_{\rm max})^{1/2} T_{\rm cond}^{13/18}}{T_{\rm reac}^{11/9}} \right) \right]^{-1} \quad \text{(C.16)}$$

and $S(x)$ is defined as

$$S(x) = \begin{cases} \left(\frac{x_h - x}{x_h - x_{\rm min,f}} \right)^{1/(6\mathrm{Sc}_R)} & \text{if } x < x_{\rm min,f} \\ 1 & \text{if } x \geq x_{\rm min,f} \end{cases} \quad \text{(C.17)}$$

References

Alexander, C. M. O. ., Newsome, S. D., Fogel, M. L., Nittler, L. R., Busemann, H., and Cody, G. D. (2010). Deuterium enrichments in chondritic macromolecular material: Implications for the origin and evolution of organics, water and asteroids. *Geochimica et Cosmochimica Acta*, **74**, 4417–4437.

Alexander, C. M. O., Bonal, L., and Sutton, S. (2012a). H Isotopes of Chondrites: Clues to the Origin of Water and Alteration Processes. *Meteoritics and Planetary Science Supplement*, **75**, 5297.

Alexander, C. M. O. D., Bowden, R., Fogel, M. L., Howard, K. T., Herd, C. D. K., and Nittler, L. R. (2012b). The Provenances of Asteroids, and Their Contributions to the Volatile Inventories of the Terrestrial Planets. *Science*, **337**, 721–.

Bai, X. and Goodman, J. (2009). Heat and Dust in Active Layers of Protostellar Disks. *ApJ*, **701**, 737–755.

Balbus, S. A. and Hawley, J. F. (1998). Instability, turbulence, and enhanced transport in accretion disks. *Reviews of Modern Physics*, **70**, 1–53.

Birnstiel, T., Dullemond, C. P., and Brauer, F. (2010). Gas- and dust evolution in protoplanetary disks. *Astronomy and Astrophysics*, **513**, A79+.

Birnstiel, T., Klahr, H., and Ercolano, B. (2012). A simple model for the evolution of the dust population in protoplanetary disks. *Astronomy & Astrophysics*, **539**, A148.

Boato, G. (1954). The isotopic composition of hydrogen and carbon in carbonaceous chondrites. *Geochimica et Cosmochimica Acta*, **6**, 209–220.

Bockelée-Morvan, D., Gautier, D., Hersant, F., Huré, J., and Robert, F. (2002). Turbulent radial mixing in the solar nebula as the source of crystalline silicates in comets. *A&A*, **384**, 1107–1118.

Bockelée-Morvan, D., Biver, N., Swinyard, B., de Val-Borro, M., Crovisier, J., Hartogh, P., Lis, D. C., Moreno, R., Szutowicz, S., Lellouch, E., Emprechtinger, M., Blake, G. A., Courtin, R., Jarchow, C., Kidger, M., Küppers, M., Rengel, M., Davis, G. R., Fulton, T., Naylor, D., Sidher, S., and Walker, H. (2012). Herschel measurements of the D/H and ^{16}O/^{18}O ratios in water in the Oort-cloud comet C/2009 P1 (Garradd). *Astronomy & Astrophysics*, **544**, L15.

Bradley, J. P. (2005). *Interplanetary Dust Particles*, chapter 1.26, pages 689–+. Elsevier B.

Brearley, A. J. (2003). Nebular versus Parent-body Processing. *Treatise on Geochemistry*, **1**, 247–268.

Briani, G., Morbidelli, A., Gounelle, M., and Nesvorný, D. (2011). Evidence for an asteroid-comet continuum from simulations of carbonaceous microxenolith dynamical evolution. *Meteoritics and Planetary Science*, **46**, 1863–1877.

Bridges, J. C., Changela, H. G., Nayakshin, S., Starkey, N. A., and Franchi, I. A. (2012). Chondrule fragments from Comet Wild2: Evidence for high temperature processing in the outer Solar System. *Earth and Planetary Science Letters*, **341**, 186–194.

Burbine, T. H., Rivkin, A. S., Noble, S. K., Mothé-Diniz, T., Bottke, W., McCoy, T. J., D. M., and A., T. C. (2008). *in Oxygen in the Solar System*, chapter 12, pages 273–343. MSA.

Cassen, P. (1996). Models for the fractionation of moderately volatile elements in the solar nebula. *Meteoritics and Planetary Science*, **31**, 793–806.

Chambers, J. E. (2009). An Analytic Model for the Evolution of a Viscous, Irradiated Disk. *ApJ*, **705**, 1206–1214.

Ciesla, F. J. and Cuzzi, J. N. (2006). The evolution of the water distribution in a viscous protoplanetary disk. *Icarus*, **181**, 178–204.

Clarke, C. J. and Pringle, J. E. (1988). The diffusion of contaminant through an accretion disc. *MNRAS*, **235**, 365–373.

Connelly, J., Bizzarro, M., Krot, A., Nordlund, A., Wielandt, D., and Ivanova, M. A. (2012). The absolute chronology and thermal processing of solids in the solar protoplanetary disk. *Science*, **338**, 651.

Cuzzi, J. N. and Zahnle, K. J. (2004). Material Enhancement in Protoplanetary Nebulae by Particle Drift through Evaporation Fronts. *The Astrophysical Journal*, **614**, 490–496.

Deloule, E., Robert, F., and Doukhan, J. C. (1998). Interstellar hydroxyl in meteoritic chondrules: implications for the origin of water in the inner solar system. *Geochimica et Cosmochimica Acta*, **62**, 3367–3378.

Desch, S. J. (2007). Mass Distribution and Planet Formation in the Solar Nebula. *ApJ*, **671**, 878–893.

Drouart, A., Dubrulle, B., Gautier, D., and Robert, F. (1999). Structure and Transport in the Solar Nebula from Constraints on Deuterium Enrichment and Giant Planets Formation. *Icarus*, **140**, 129–155.

Dubrulle, B. and Frisch, U. (1991). Eddy viscosity of parity-invariant flow. *Phys. Rev. A*, **43**, 5355–5364.

Engrand, C. and Maurette, M. (1998). Carbonaceous micrometeorites from Antarctica. *Meteoritics and Planetary Science*, **33**, 565–580.

Fleming, T. and Stone, J. M. (2003). Local Magnetohydrodynamic Models of Layered Accretion Disks. *ApJ*, **585**, 908–920.

Gail, H.-P. (2001). Radial mixing in protoplanetary accretion disks. I. Stationary disc models with annealing and carbon combustion. *Astronomy & Astrophysics*, **378**, 192–213.

Gammie, C. F. (1996). Layered Accretion in T Tauri Disks. *ApJ*, **457**, 355–362.

Garaud, P. (2007). Growth and migration of solids in evolving protostellar disks. i. methods and analytical tests. *ApJ*, **671**, 2091–2114.

Geiss, J. and Gloeckler, G. (2003). Isotopic Composition of H, HE and NE in the Protosolar Cloud. *Space Science Reviews*, **106**, 3–18.

Ghosh, A., Weidenschilling, S. J., McSween, Jr., H. Y., and Rubin, A. (2006). *Asteroidal Heating and Thermal Stratification of the Asteroidal Belt*, pages 555–566.

Gounelle, M., Engrand, C., Alard, O., Bland, P. A., Zolensky, M. E., Russell, S. S., and Duprat, J. (2005). Hydrogen isotopic composition of water from fossil micrometeorites in howardites. *Geochimica et Cosmochimica Acta*, **69**, 3431–3443.

Gounelle, M., Morbidelli, A., Bland, P. A., Spurny, P., Young, E. D., and Sephton, M. (2008). *Meteorites from the Outer Solar System?*, pages 525–541.

Grimm, R. E. and McSween, Jr., H. Y. (1989). Water and the thermal evolution of carbonaceous chondrite parent bodies. *Icarus*, **82**, 244–280.

Hartmann, L., Calvet, N., Gullbring, E., and D'Alessio, P. (1998). Accretion and the Evolution of T Tauri Disks. *ApJ*, **495**, 385–400.

Hartogh, P., Lis, D. C., Bockelée-Morvan, D., de Val-Borro, M., Biver, N., Küppers, M., Emprechtinger, M., Bergin, E. A., Crovisier, J., Rengel, M., Moreno, R., Szutowicz, S., and Blake, G. A. (2011). Ocean-like water in the Jupiter-family comet 103P/Hartley 2. *Nature*, **478**, 218–220.

Hayashi, C. (1981). Structure of the Solar Nebula, Growth and Decay of Magnetic Fields and Effects of Magnetic and Turbulent Viscosities on the Nebula. *Progress of Theoretical Physics Supplement*, **70**, 35–53.

Hersant, F., Gautier, D., and Huré, J.-M. (2001). A Two-dimensional Model for the Primordial Nebula Constrained by D/H Measurements in the Solar System: Implications for the Formation of Giant Planets. *ApJ*, **554**, 391–407.

Ilgner, M. and Nelson, R. P. (2008). Turbulent transport and its effect on the dead zone in protoplanetary discs. *Astronomy & Astrophysics*, **483**, 815–830.

Jacquet, E., Fromang, S., and Gounelle, M. (2011). Radial transport of refractory inclusions and their preservation in the dead zone. *A&A*, **526**, L8.

Jacquet, E., Gounelle, M., and Fromang, S. (2012). On the aerodynamic redistribution of chondrite components in protoplanetary disks. *Icarus*, **220**, 162–173.

Johansen, A., Klahr, H., and Mee, A. J. (2006). Turbulent diffusion in protoplanetary discs: the effect of an imposed magnetic field. *MNRAS*, **370**, L71–L75.

Kerridge, J. F. (1985). Carbon, hydrogen and nitrogen in carbonaceous chondrites Abundances and isotopic compositions in bulk samples. *Geochimica et Cosmochimica Acta*, **49**, 1707–1714.

Kita, N. T. and Ushikubo, T. (2012). Evolution of protoplanetary disk inferred from ^{26}Al chronology of individual chondrules. *Meteoritics and Planetary Science*, **47**, 1108–1119.

Kleine, T., Touboul, M., van Orman, J. A., Bourdon, B., Maden, C., Mezger, K., and Halliday, A. N. (2008). Hf W thermochronometry: Closure temperature and constraints on the accretion and cooling history of the H chondrite parent body. *Earth and Planetary Science Letters*, **270**, 106–118.

Kolodny, Y., Kerridge, J. F., and Kaplan, I. R. (1980). Deuterium in carbonaceous chondrites. *Earth and Planetary Science Letters*, **46**, 149–158.

Lathrop, D. P., Fineberg, J., and Swinney, H. L. (1992). Transition to shear-driven turbulence in couette-taylor flow. *Phys. Rev. A*, **46**, 6390–6405.

Lécluse, C. and Robert, F. (1994). Hydrogen isotope exchange reaction rates: Origin of water in the inner solar system. *Geochimica et Cosmochimica Acta*, **58**, 2927–2939.

Lécuyer, C., Gillet, P., and Robert, F. (1998). The hydrogen isotope composition of seawater and the global water cycle. *Chemical Geology*, **145**, 249–261.

McCanta, M. C., Treiman, A. H., Dyar, M. D., Alexander, C. M. O. ., Rumble, III, D., and Essene, E. J. (2008). The LaPaz Icefield 04840 meteorite: Mineralogy, metamorphism, and origin of an amphibole- and biotite-bearing R chondrite. *Geochimica et Cosmochimica Acta*, **72**, 5757–5780.

McNaughton, N. J., Hinton, R. W., Pillinger, C. T., and Fallick, A. E. (1982). D/H Ratios of Some Ordinary and Carbonaceous Chondrites. *Meteoritics*, **17**, 252.

Mousis, O., Gautier, D., Bockelée-Morvan, D., Robert, F., Dubrulle, B., and Drouart, A. (2000). Constraints on the Formation of Comets from D/H Ratios Measured in H_2O and HCN. *Icarus*, **148**, 513–525.

Oishi, J. S. and Mac Low, M.-M. (2009). On Hydrodynamic Motions in Dead Zones. *ApJ*, **704**, 1239–1250.

Pearson, V. K., Sephton, M. A., Gilmour, I., and Franchi, I. A. (2001). Hydrogen Isotopic Composition of the Tagish Lake Meteorite: Comparison with Other Carbonaceous Chondrites. In *Lunar and Planetary Institute Science Conference Abstracts*, volume 32 of *Lunar and Planetary Institute Science Conference Abstracts*, page 1861.

Piani, L. (2012). *Origine des éléments volatils dans le système solaire*. Ph.D. thesis, Muséum National d'Histoire Naturelle.

Piani, L., Rémusat, L., and Robert, F. (2012). Determination of the h isotopic composition of individual components in fine-scale mixtures of organic matter and phyllosilicates with the nanoscale secondary ion mass spectrometry. *Analytical chemistry*, **84**, 10199–10206.

Prinn, R. G. (1990). On neglect of nonlinear momentum terms in solar nebula accretion disk models. *ApJ*, **348**, 725–729.

Remusat, L., Guan, Y., Wang, Y., and Eiler, J. M. (2010). Accretion and Preservation of D-rich Organic Particles in Carbonaceous Chondrites: Evidence for Important Transport in the Early Solar System Nebula. *The Astrophysical Journal*, **713**, 1048–1058.

Remusat, L., Bernard, S., Le Guillou, C., and Brearley, A. (2011). Parent Body Influence on Organic Matter: The Message from Paris. *Meteoritics and Planetary Science Supplement*, **74**, 5327.

Richet, P., Bottinga, Y., and Janoy, M. (1977). A review of hydrogen, carbon, nitrogen, oxygen, sulphur, and chlorine stable isotope enrichment among gaseous molecules. *Annual Review of Earth and Planetary Sciences*, **5**, 65–110.

Robert, F. (2006). *Solar System Deuterium/Hydrogen Ratio*, pages 341–351.

Robert, F. and Epstein, S. (1982). The concentration and isotopic composition of hydrogen, carbon and nitrogen in carbonaceous meteorites. *Geochimica et Cosmochimica Acta*, **46**, 81–95.

Scott, E. R. D. and Krot, A. N. (2003). Chondrites and their Components. *Treatise on Geochemistry*, **1**, 143–200.

Stevenson, D. J. (1990). Chemical heterogeneity and imperfect mixing in the solar nebula. *The Astrophysical Journal*, **348**, 730–737.

Terquem, C. E. J. M. L. J. (2008). New Composite Models of Partially Ionized Protoplanetary Disks. *ApJ*, **689**, 532–538.

Turner, N. J., Carballido, A., and Sano, T. (2010). Dust Transport in Protostellar Disks Through Turbulence and Settling. *ApJ*, **708**, 188–201.

Villeneuve, J., Chaussidon, M., and Libourel, G. (2009). Homogeneous distribution of aluminum-26 in the solar system from the magnesium isotopic composition of chondrules. *Science*, **325**, 985–988.

Walsh, K. J., Morbidelli, A., Raymond, S. N., O'Brien, D. P., and Mandell, A. M. (2011). A low mass for Mars from Jupiter's early gas-driven migration. *Nature*, **475**, 206–209.

Weidenschilling, S. J. (2004). *From icy grains to comets*, pages 97–104.

Wozniakiewicz, P. J., Bradley, J. P., Ishii, H. A., Brownlee, D. E., Kearsley, A. T., Burchell, M. J., and Price, M. C. (2012). Grain Sorting in Cometary Dust from the Outer Solar Nebula. *Astrophysical Journal Letters*, **760**, L23.

Yang, J. and Epstein, S. (1983). Interstellar organic matter in meteorites. *Geochimica et Cosmochimica Acta*, **47**, 2199–2216.

Yang, L. and Ciesla, F. J. (2012). The effects of disk building on the distributions of refractory materials in the solar nebula. *Meteoritics and Planetary Science*, **47**, 99–119.

Yang, L., Ciesla, F. J., and Alexander, C. M. O. (2012). The D/H Ratio of Water in a Forming and Evolving Protoplanetary Disk. In *Lunar and Planetary Institute Science Conference Abstracts*, volume 43 of *Lunar and Planetary Institute Science Conference Abstracts*, page 2023.

Youdin, A. N. and Lithwick, Y. (2007). Particle stirring in turbulent gas disks: Including orbital oscillations. *Icarus*, **192**, 588–604.

Zhu, Z., Hartmann, L., and Gammie, C. (2010). Long-term Evolution of Protostellar and Protoplanetary Disks. II. Layered Accretion with Infall. *ApJ*, **713**, 1143–1158.

Zolensky, M. E., Zega, T. J., Yano, H., Wirick, S., Westphal, A. J., Weisberg, M. K., Weber, I., Warren, J. L., Velbel, M. A., Tsuchiyama, A., Tsou, P., Toppani, A., Tomioka, N., Tomeoka, K., Teslich, N., Taheri, M., Susini, J., Stroud, R., Stephan, T., Stadermann, F. J., Snead, C. J., Simon, S. B., Simionovici, A., See, T. H., Robert, F., Rietmeijer, F. J. M., Rao, W., Perronnet, M. C., Papanastassiou, D. A., Okudaira, K., Ohsumi, K., Ohnishi, I., Nakamura-Messenger, K., Nakamura, T., Mostefaoui, S., Mikouchi, T., Meibom, A., Matrajt, G., Marcus, M. A., Leroux, H., Lemelle, L., Le, L., Lanzirotti, A., Langenhorst, F., Krot, A. N., Keller, L. P., Kearsley, A. T., Joswiak, D., Jacob, D., Ishii, H., Harvey, R., Hagiya, K., Grossman, L., Grossman, J. N., Graham, G. A., Gounelle, M., Gillet, P., Genge, M. J., Flynn, G., Ferroir, T., Fallon, S., Ebel, D. S., Dai, Z. R., Cordier, P., Clark, B., Chi, M., Butterworth, A. L., Brownlee, D. E., Bridges, J. C., Brennan, S., Brearley, A., Bradley, J. P., Bleuet, P., Bland, P. A., and Bastien, R. (2006). Mineralogy and Petrology of Comet 81P/Wild 2 Nucleus Samples. *Science*, **314**, 1735–1739.

Zsom, A., Ormel, C. W., Güttler, C., Blum, J., and Dullemond, C. P. (2010). The outcome of protoplanetary dust growth: pebbles, boulders, or planetesimals? II. Introducing the bouncing barrier. *A&A*, **513**, A57+.